A Solid-State NMR, X-ray Diffraction, and ab Initio Computational Study of Hydrogen-Bond Structure and Dynamics of Pyrazole-4-Carboxylic Acid Chains

Concepción Foces-Foces,[†] Aurea Echevarría,[‡] Nadine Jagerovic,[‡] Ibon Alkorta,[‡] José Elguero,*[,‡] Uwe Langer,[§] Oliver Klein,[§] María Minguet-Bonvehí,[§] and Hans-Heinrich Limbach*[,§]

Contribution from the Departamento de Cristalografía, Instituto de Química-Física 'Rocasolano', CSIC, Serrano, 119, E-28006 Madrid, Spain, the Instituto de Química Médica, CSIC, Juan de la Cierva 3, E-28006 Madrid, Spain, and the Institut für Chemie, Freie Universität Berlin, Takustrasse 3, D-14195 Berlin, Germany

Received July 20, 2000. Revised Manuscript Received April 30, 2001

Abstract: Using high-resolution solid-state ^{15}N CMAS NMR, X-ray crystallography, and ab initio calculations, we have studied the structure of solid pyrazole-4-carboxylic acid (**1**). The crystal structure was determined at 295 and 150 K. Molecules of **1** are located on a two-fold axis, implying proton disorder of the NH and OH groups; no phase transition was observed between these two temperatures. The compound forms quasi-linear ribbons in which the molecules are linked by cyclic hydrogen bonds between pyrazole and carboxylic acid groups with disordered hydrogen-bonded protons. Crystallography is unable to decide whether the disorder is dynamic or static. NMR shows that this disorder is dynamic, that is, consisting of very fast degenerate double proton transfers between two rapidly interconverting O−H···N and O···H−N hydrogen bridges. However, at low temperature, NMR shows a proton disorder−order transition where the protons are preferentially localized on given nitrogen and oxygen atoms. An amorphous phase exhibiting proton order is observed when the compound is precipitated rapidly. In this case, the defects are annealed by moderate heating. Ab initio calculations performed on oligomers of **1** show that the O−H···N hydrogen bridge is about 0.064 Å shorter and less bent (∼171°) than the O···H−N hydrogen bridge (∼150°). For an isolated ribbon, this result leads to structures with localized protons, either to a cycle with about 200 molecules, or to a quasi-linear ribbon involving an undulated structure, or to a combination of both motifs. Only the undulated structure is compatible with the linear ribbon observed by X-ray crystallography, where the fast proton transfer in the high-temperature phase is assisted by the motions of the undulated chain. A disordered structure is assigned to the amorphous phase, which exhibits the combination of the curved and the undulated motifs.

Introduction

Coupled hydrogen-bonded networks with mobile protons are important elements of supramolecular reactivity in chemistry and biology. Unfortunately, these phenomena are very complex and require the study of model systems. In recent years, some of us have demonstrated that solid pyrazoles represent such a class of model systems.[1−5] Depending on the substituents, these molecules form either linear chains such as the parent compound pyrazole,[1] or cyclic dimers, trimers, or tetramers[2−5] as depicted in Figure 1. Whereas in the linear chains the protons are ordered and immobile,[1b] the cyclic complexes generally form two degenerate states A and B, which interconvert via fast double, triple, or quadruple proton transfers in the millisecond to second time scale, as has been shown using dynamic high-resolution solid-state ^{13}C and ^{15}N CPMAS NMR spectroscopy.[2−5] Accurate rate constants of the proton motions, including the multiple kinetic hydrogen/deuterium isotope effects in a wide temperature range, can be obtained using ^{15}N NMR line shape analysis and magnetization transfer experiments.[5] For the triple proton transfers, such studies revealed a concerted process via a

[†] Departamento de Cristalografía, Instituto de Química-Física 'Rocasolano'.

[‡] Instituto de Química Médica.

[§] Institut für Chemie, Freie Universität Berlin.

(1) (a) La Cour, T.; Rasmussen, S. E., *Acta Chem. Scand.* **1973**, *27*, 1845. (b) Elguero, J.; Fruchier, A.; Pellegrin, V. *J. Chem. Soc., Chem. Commun.* **1981**, 1207.

(2) (a) Baldy, A.; Elguero, J.; Faure, R.; Pierrot, M.; Vincent, E.-J. *J. Am. Chem. Soc.* **1985**, *107*, 5290. (b) Smith, J. A. S.; Wehrle, B.; Aguilar-Parrilla, F.; Limbach, H.-H.; Foces-Foces, C.; Cano, F. H.; Elguero, J.; Baldy, A.; Pierrot, M.; Khurshid, M. M. T.; Larcombe-McDouall, J. B. *J. Am. Chem. Soc*. **1989**, *111*, 7304. (c) Aguilar-Parrilla, F.; Scherer, G.; Limbach, H.-H.; Foces-Foces, C.; Cano, F. H.; Smith, J. A. S.; Toiron, C.; Elguero, J. *J. Am. Chem. Soc*. **1992**, *114*, 9657. (d) Llamas-Saiz, A. L.; Foces-Foces, C.; Cano, F. H.; Jimenez, P.; Laynez, J.; Meutermans, W.; Elguero, J.; Limbach, H. H.; Aguilar-Parrilla, F. *Acta Crystallogr*. **1994**, *B50*, 746. (e) Aguilar-Parrilla, F.; Limbach, H. H.; Foces-Foces, C.; Cano, F. H.; Jagerovic, N.; Elguero, J. *J. Org. Chem.* **1995**, *60*, 1965. (f) Hoelger, C.; Limbach, H.-H.; Aguilar-Parrilla, F.; Elguero, J.; Weintraub, O.; Vega, S. *J. Magn. Res.* **1996**, *A120*, 46. (g) Foces-Foces, C.; Llamas-Saiz, A. L.; Elguero, J. *Z. Kristallogr*. **1999**, *214*, 237. (h) Catalan, J.; Abboud, J. L. M.; Elguero, J. *Adv. Heterocycl. Chem.* **1987**, *41*, 187. (i) Alkorta, I.; Elguero, J.; Donnadieu, B.; Etienne, M.; Jaffart, J.; Schagen, D.; Limbach, H.-H. *New J. Chem*. **1999**, *23*, 1231.

(3) (a) Toda, F.; Tanaka, K.; Foces-Foces, C.; Llamas-Saiz, A. L.; Limbach, H.-H.; Aguilar-Parrilla, F.; Claramunt, R. M.; Lopez, C.; Elguero, J. *J. Chem. Soc., Chem. Commun.* **1993**, 1139. (b) Aguilar-Parrilla, F.; Claramunt, R. M.; Lopez, C.; Sanz, D.; Limbach, H.-H.; Elguero J. *J. Phys. Chem.* **1994**, *98*, 8752.

(4) de Paz, J. L. G.; Elguero, J.; Foces-Foces, C.; Llamas-Saiz, A. L.; Aguilar-Parrilla, F.; Klein, O.; Limbach, H.-H. *J. Chem. Soc., Perkin Trans. 2* **1997**, 101.

(5) (a) Aguilar-Parrilla, F.; Klein, O.; Elguero, J.; Limbach, H.-H. *Ber. Bunsen-Ges. Phys. Chem*. **1997**, *101*, 889. (b) Klein, O.; Bonvehi, M. M.; Aguilar-Parrilla, F.; Elguero, J.; Limbach, H.-H. *Isr. J. Chem.* **1999**, *34*, 291.

10.1021/ja002688l CCC: $20.00 © 2001 American Chemical Society
Published on Web 07/20/2001

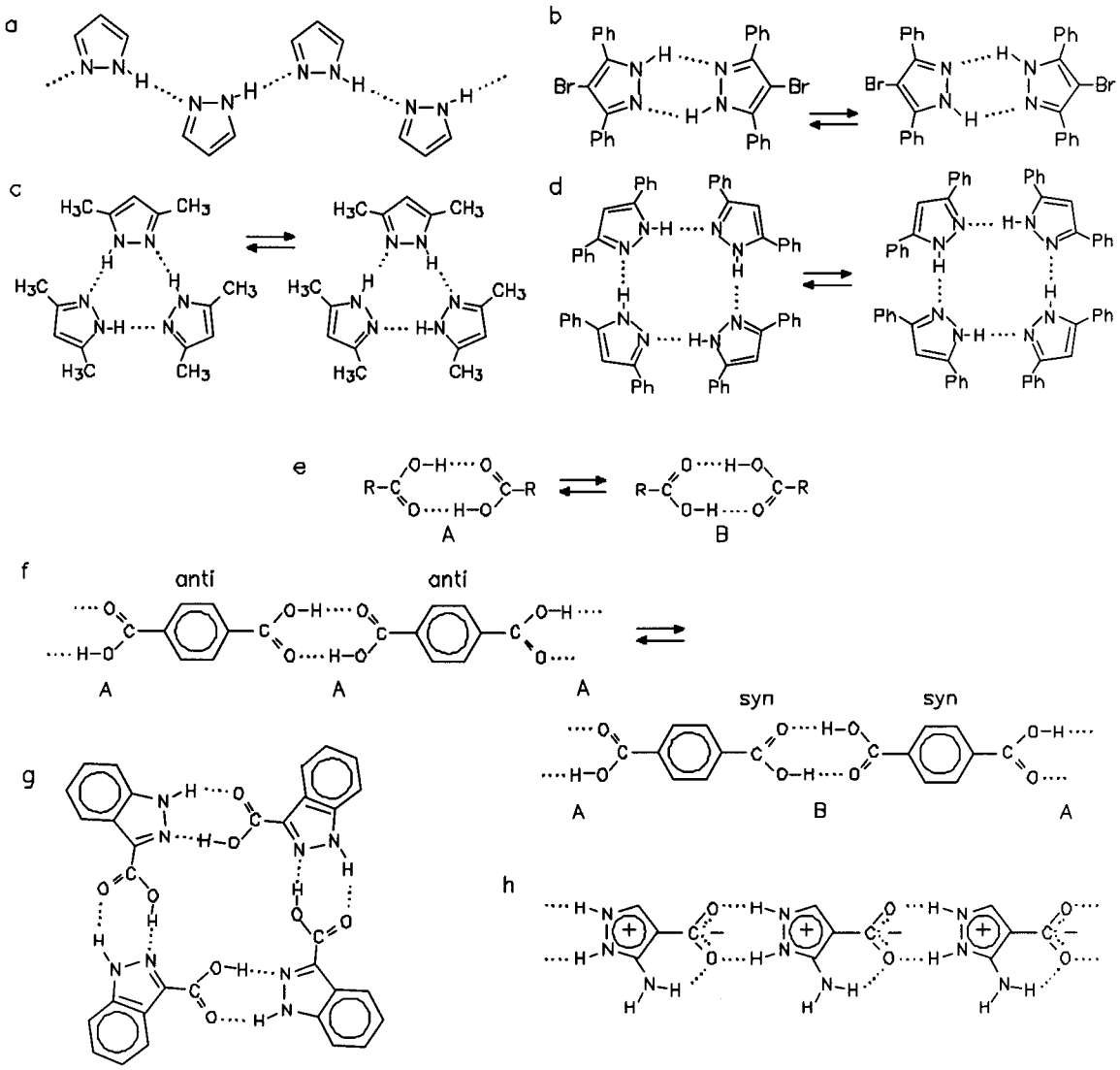

Figure 1. Hydrogen-bonded networks and proton tautomerism of pyrazoles (a) to (d), monofunctional (e) and bifunctional carboxylic acids (f), 1*H*-indazole-3-carboxylic acid (g) and 2-aminopyrazolecarboxylic acid (h). For further explanation see text.

hydrogen bond compressed transition state, with strong tunneling contributions at low temperatures.[5]

In contrast to N−H···N hydrogen bonds, the related O−H···O hydrogen bonds are generally much stronger. Thus, it is not surprising that the double proton transfer dynamics between forms A and B in the related, well-studied carboxylic acid dimers (Figure 1e) are much faster, generally in the microsecond to nanosecond time scale as manifested in the longitudinal ^{1}H and ^{2}H NMR relaxation of these molecules.[6] The interest in carboxylic acid also stems from the finding that this group is one of the most important motifs used in organic crystal engineering for self-assembling of organic molecular building blocks.[7] Much less is known about the proton dynamics in such extended networks. As an example, we discuss the case of *p*-terephthalic acid, which consists of linear ribbons of covalently linked cyclic carboxylic acid dimers (Figure 1f). Using ^{1}H NMR spectroscopy and relaxometry, Fischer et al.[8] revealed that the formation of the ribbons does not suppress the proton dynamics. These authors observed a slightly asymmetric double minimum potential for the proton dynamics, exhibiting a free enthalpy difference of 1.8 kJ mol^{-1}, and a time scale of the proton motion in the microsecond- to nanosecond range, which is similar to that of the carboxylic acid dimers.[6] Upon cooling the sample, a proton disorder−order transition was observed at 80 K.

As a consequence of the above considerations, an interesting situation arises if one constructs molecules exhibiting both the acid carboxylic and the basic pyrazole groups. In this case, these

(6) (a) Meier, B. H.; Graf, F.; Ernst, R. R. *J. Chem. Phys.* **1982**, *76*, 768. (b) Meyer, R.; Ernst, R. R. *J. Chem. Phys.* **1990**, *93*, 768. (c) Heuer, A.; Haeberlen, U. *J. Chem. Phys.* **1991**, *95*, 4201. (d) Stöckli, A.; Maier, B. H.; Kreis, R.; Meyer, R.; Ernst, R. R. *J. Chem. Phys.* **1990**, *93*, 15002. (e) Horsewill, A. J.; Brougham, D. F.; Jenkinson, R. I.; McGloin, C. J.; Trommsdorff, H. P.; Johnson, M. R. *Ber. Bunsen-Ges. Phys. Chem.* **1998**, *102*, 317. (f) Neumann, M. A.; Craciun, S.; Corval, A.; Johnson, M. R.; Horsewill, A. J.; Benderskii, V. A.; Trommsdorff, H. P. *Ber. Bunsen-Ges. Phys. Chem.* **1998**, *102*, 325. (g) Loerting, T.; Liedl, K. R. *J. Am. Chem. Soc.* **1998**, *120*, 12595.

(7) (a) Allen, F. H.; Motherwell, W. D. S.; Raithby, P. R.; Shields, G. P.; Taylor, R. *New J. Chem.* **1999**, 25−34. (b) Desiraju, G. R. *Crystal Engineering. The Design of Organic Solids*; Elsevier: Amsterdam, 1989; pp 129−132. (c) Bernstein, Etter, M. C.; Leiserowitz, L. The Role of Hydrogen Bonding in Molecular Assemblies. In *Structure Correlation*; Bürgi, H. B., Dunitz, J. D., Eds.; VCH: Weinheim, 1994; Vol. 2, pp 447−450. (d) Weber, E. Shape and Symmetry in the Design of New Hosts. In *Comprehensive Supramolecular Chemistry*: Atwood, J. L., Davies, J. E. D., Macnicol, D. D., Vögtle, F., Eds.; 1996; Vol. 6, pp 535−592. (e) Thalladi, V. R.; Goud, B. S.; Hoy, V. J.; Allen, F. H.; Howard, J. A, K.; Desiraju, G. R. *Chem. Commun.* **1996**, 401. (f) Meot-Ner (Mautner), M.; Elmore, D. E.; Scheiner, S. *J. Am. Chem. Soc.* **1999**, *121*, 7625−7635.

(8) Fischer, P. Z.; Maier, B. H.; Ernst, R. R.; Hewat, A. W.; Jorgensen, J. D.; Rotella, F. J. *J. Solid State Chem.* **1986**, *61*, 20.

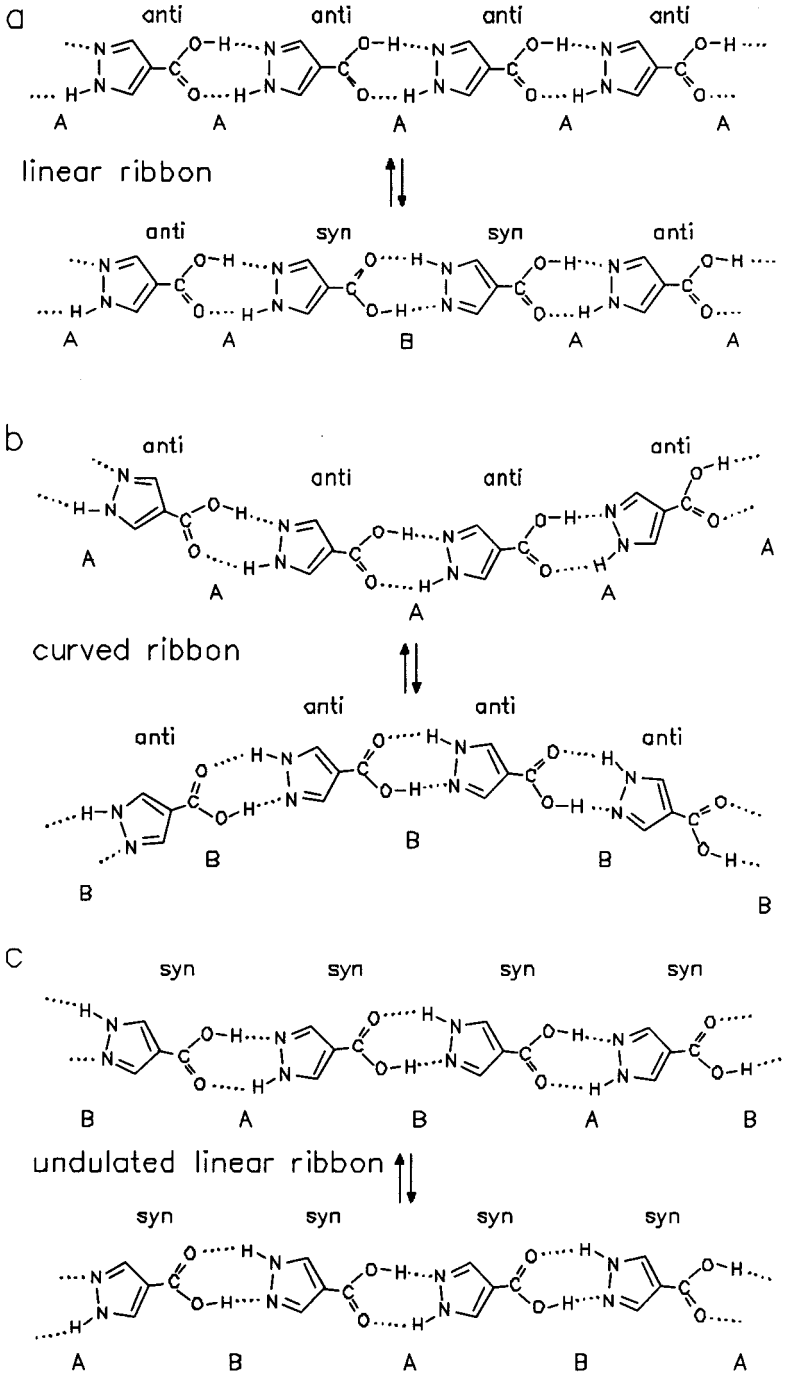

Figure 2. Potential supramolecular structure and tautomeric states of ribbons of pyrazole-4-carboxylic acid (**1**). (a) Linear Ribbon. (b) Arcs or Cycles. (c) Undulated ribbon.

groups could form either cyclic homodimers with OHO and NHN hydrogen bonds or heterodimers with OHN hydrogen bonds, where the proton dynamics are intermediate between the carboxylic acid and pyrazole dimers. On the other hand, the carboxylic acid groups can be expected to act as an acid and the pyrazole groups as a base. Evidence for such a situation was obtained recently by X-ray diffraction of 2-aminopyrazole-carboxylic acid, which forms a zwitterionic ribbon in the solid state with two O···H−N hydrogen bonds,[9] as depicted in Figure 1g. On the other hand, the acid−base interaction is much weaker in 1*H*-indazole-3-carboxylic acid, which forms a tetramer supercycle with four pyrazole-carboxylic acid links.[10] Finally, we would like to mention that Bureiko et al. have reported solution studies of the double proton transfer between carboxylic acids and *N*-unsubstituted pyrazoles.[11] These encouraged us to look for cocrystals of the two components. We found that 3,5-dimethylpyrazole is able to form cocrystals with 2,4,6-trimethylbenzoic acid. However, these do not show any sign of proton disorder.[12]

In recent years, in our search for systems in which both anchoring groups exhibit a solid-state proton tautomerism we have studied one of the simplest compounds of this series, that is, pyrazole-4-carboxylic acid **1** (Figure 2). Although **1** was

(9) Benetollo, F.; Del Para, A. *Acta Crystallogr., Sect. C* **1993**, *49*, 779.
(10) Dobson, A. J.; Gerkin, R. E. *Acta Crystallogr., Sect. C* **1998**, *54*, 253.
(11) Bureiko, S. F.; Golubev, N. S.; Chernysheva, I. V. *Khim. Fiz.* **1987**, *6*, 176.
(12) Foces-Foces, C.; Infantes, L.; Aguilar-Parrilla, F.; Golubev, N. S.; Limbach, H.-H.; Elguero, J. *J. Chem. Soc., Perkin Trans. 2* **1996**, 349.

synthesized a long time ago,[13] neither the crystal structure nor NMR measurements have been reported for this molecule. At first sight, one would predict for this molecule a linear molecular ribbon in the solid state, linked by two coupled O−H···N− and N−H···O− hydrogen bridges with equal oxygen···nitrogen distances, as depicted in Figure 2a, where each coupled bridge can exhibit the two tautomeric states A and B. In principle, the energies of A and B depend on the state of the neighboring pyrazole-carboxylic acid units. On average the two states should be degenerate. However, if an arrangement where the O−H···N hydrogen bridge is somewhat shorter—or simply more linear—than the O···H−N hydrogen bridge and it is energetically favored as compared to bridges with equal geometries, the molecular ribbon will no longer be linear. In Figure 2b we have depicted schematically the case where all molecules adopt an *anti*-conformation with respect to the two mobile protons, that is where all proton transfer units of a chain exhibit the same tautomeric states. Such ribbons should exhibit a curvature and will lead to cycles with a large, thus far unknown, number of molecules. Thus, a proton tautomerism between ...AAAAA... and ...BBBBB... requires major molecular motions between two differently curved ribbons that are precluded in the solid state. A local interconversion from ...AAAAA... to ...AABAA... will also require a molecular rearrangement, or it will be energetically unfavorable. On the other hand, when all molecules adopt a *syn*-conformation, a quasi-linear "undulated" ribbon should result, exhibiting an alternation of the tautomeric states ...ABABA... Again, the interconversion to ...BABAB... corresponds to a twist of the undulated form, for which the whole ribbon will need to be rearranged. The formation of "defects" like ...ABBBA... will also be a nondegenerate process.

To try to find answers to the above questions, we carried out a number of experiments and calculations that will be reported in this paper. After an Experimental Section, we will describe the X-ray crystal structure of **1**, which corresponds to a situation in which the *anti* and *syn* conformations are equally populated. We then describe the results of variable temperature ^{15}N CPMAS NMR measurements on ^{15}N-labeled **1**, whose synthesis is also reported. The NMR measurements provide evidence for proton disorder, in agreement with the crystal structure. However, at low temperatures a complex transition to a proton ordered state is observed by NMR, which we ascribe to the formation of an undulated form according to Figure 2c. Moreover, an amorphous metastable form of **1** has been observed with a mixture of ordered and disordered protons at room temperature, which we ascribe to a "polymer" consisting of a combination of various cyclic and undulated conformations. Finally, to help interpret the experimental results, we carried out high-level ab initio calculations of various associates of **1**. These calculations give indications concerning the coupling of neighboring pyrazole-carboxylic acid linkages and indeed predict supercyclic or undulated structures for larger associates of **1**.

Experimental Section

Synthesis of ^{15}N-Labeled Pyrazole-Carboxylic Acid 1. The synthesis of pyrazole-4-carboxylic acid-$^{15}N_2$ was carried out by minor modification of the synthesis of the nonlabeled compound.[13] In a first step, 4-methylpyrazole is prepared from hydrazinium sulfate and methylmalonaldehyde diethyl acetal.[13a] Here, the ^{15}N-labeled hydrazinium sulfate (95% enrichment) was obtained from Chemotrade, Leipzig, Germany. In a second step, the product is oxidized into **1**.[13b] Total yield (from hydrazinium sulfate-$^{15}N_2$) is about 37%. Transparent colorless crystals of pyrazole-4-carboxylic acid were obtained by slow evaporation of water−ethanol solutions.

X-ray Diffraction and DSC Measurements. A transparent colorless crystal with appoximate dimensions 0.27 mm × 0.33 mm × 0.40 mm was used to collect X-ray data ($\lambda = 1.5418$ Å) on a Seifert XRD3000-S[15] and a Philips PW1100[16] four circles diffractometer, respectively. Using an Oxford Cryostream device,[14] two sets of data were collected, one at 295 K and the other at 150 K. The stated temperatures were measured continuously during data collection. The structure was solved at room temperature by direct methods (SIR97)[17] and refined at room- and at low temperature by least-squares procedures on F_{obs}. The weighting schemes were established[18] empirically so as to give no trends in $\langle w\Delta^2F\rangle$ vs $\langle F_o\rangle$ or $\langle \sin\theta/\lambda\rangle$: $w = K/[([a + b]F_o)^2][c + (d[\sin\theta]/)\lambda]$; the *a, b, c* and *d* parameters were adjusted to flatten the initial trends. The scattering factors were taken from the International Tables for X-ray Crystallography.[19] Most of the calculations were performed using the Xtal 3.6 system[20] of programs and PARST.[21] The CIF files were deposited with the Cambridge Crystallographic Data Center (CCDC 139857 and 139858).

Differential scanning calorimetry experiments of **1** were performed using a Mettler GraphWare instrument.

Ab Initio Calculations. All of the calculations have been carried out with the Gaussian-94[22] and Gaussian-98[22] programs at the B3LYP/6-31G* level of theory.[23]

The two 4-pyrazole-carboxylic acid monomers and the four possible dimers (the total number of different structures is 2^n, where n is the number of monomers for each cluster) have been fully optimized, and frequency calculations have been carried out to confirm the minimum nature of the structures obtained. In all of the cases, they have C_s symmetry. For the rest of the complexes, this symmetry has been assumed, and no frequency calculations were carried out.

All of the possible trimers (eight) and eight tetramers that correspond to the proton-transfer configurations that can be obtained using AAAAA

(13) Synthesis of pyrazole-4-carboxylic acid. (a) 4-Methylpyrazole from hydrazine sulfate and methylmalonaldehyde diethyl acetal. (b) Oxidation to **1**.

(14) Cosier, J.; Glazer, A. M. *J. Appl. Crystallogr*. **1986**, *19*, 105.
(15) Seifert, *CRYSOM*, Version 2.8.; Seifert, u.Co.: Ahrensburg, Germany, 1996.
(16) Hornstra, J.; Vossers, H. *Philips Tech. Rev.* **1973**, *33*, 61.
(17) Altomare, A.; Cascarano, G.; Giacovazzo, C.; Guagliardi, A.; Moliterni, A. G. G.; Burla, M. C.; Polidori, G.; Camalli, M.; Spagna, R. *SIR97*, A Package for Crystal Structure Solution by Direct methods and Refinement; University of Bari, Italy, 1997.
(18) Martinez-Ripoll, M.; Cano, F. H. *PESOS*, Unpublished Program; Instituto "Rocasolano": CSIC, Madrid, Spain, 1975.
(19) *International Tables for X-ray Crystallography*; Kynoch Press: Birmingham, England, 1974.
(20) Hall, S. R., du Boulay, D. J., Olthof-Hazekamp, R., Eds. *The Xtal System of Crystallographic Software. Xtal3.6; User's Manual*; The University of Western Australia: Australia, 1999.
(21) Nardelli. M. *Comput. Chem.* **1983**, *7*, 95.
(22) Frisch, M. J.; Trucks, G. W.; Schlegel, H. B.; Gill, P. M. W.; Johnson, B. G.; Robb, M. A.; Cheeseman, J. R.; Keith, T.; Petersson, G. A.; Montgomery, J. A.; Raghavachari, K.; Al-Laham, M. A.; Zakrzewski, V. G.; Ortíz, J. V.; Foresman, J. B.; Peng, C. Y.; Ayala, P. Y.; Chen, W.; Wong, M. W.; Andres, J. L.; Replogle, E. S.; Gomperts, R.; Martin, R. L.; Fox, D. J.; Binkley, J. S.; Defrees, D. J.; Baker, J.; Stewart, J. P.; Head-Gordon, M.; González, C.; Pople, J. A. *Gaussian 94*, revision E.2; Gaussian, Inc.: Pittsburgh, PA, 1995. Frisch, M. J.; Trucks, G. W.; Schlegel, H. B.; Scuseria, G. E.; Robb, M. A.; Cheeseman, J. R.; Zakrzewski, V. G.; Montgomery, J. A.; Stratmann, R. E.; Burant, J. C.; Dapprich, S.; Millam, J. M.; Daniels, A. D.; Kudin, K. N.; Strain, M. C.; Farkas, O.; Tomasi, J.; Barone, V.; Cossi, M.; Cammi, R.; Mennucci, B.; Pomelli, C.; Adamo, C.; Clifford, S.; Ochterski, J.; Petersson, G. A.; Ayala, P. Y.; Cui, Q.; Morokuma, K.; Malick, D. K.; Rabuck, A. D.; Raghavachari, K.; Foresman, J. B.; Cioslowski, J.; Ortiz, J. V.; Stefanov, B. B.; Liu, G.; Liashenko, A.; Piskorz, P.; Komaromi, I.; Gomperts, R.; Martin, R. L.; Fox, D. J.; Keith, T.; Al-Laham, M. A.; Peng, C. Y.; Nanayakkara, A.; Gonzalez, C.; Challacombe, M.; Gill, P. M. W.; Johnson, B. G.; Chen, W.; Wong, M. W.; Andres, J. L.; Head-Gordon, M.; Replogle, E. S.; Pople, J. A. *Gaussian 98*; Gaussian, Inc.: Pittsburgh, PA, 1998.
(23) B3LYP: Becke, A. D. *Phys. Rev. A* **1988**, *38*, 3098. Becke, A. D. *J. Chem. Phys.* **1993**, *98*, 5648; Lee, C.; Yang, W.; Parr, R. G. *Phys. Rev. B* **1988**, *37*, 785. Miehlich, B. Savin, A.; Stoll, H.; Preuss, H. *Chem. Phys. Lett*. **1989**, *157*, 200; Parr, R. G.; Yang, W. *Density-Functional Theory of Atoms and Molecules*; Oxford: New York, 1989; Bartolotti, L. J.; Fluchick, K. *Reviews in Computational Chemistry*; Lipkowitz, K. B., Boyd, D. B., Eds.; VCH Publishers: New York, 1996; Vol. 7, pp 187−216. 6-31G*: Hariharan, P. C.; Pople, J. A. *Theor. Chim. Acta* **1973**, *28*, 213.

as the initial structure were studied. Finally, two pentamers and two heptamers were considered.

^{15}N Solid-State NMR Spectroscopy of Pyrazole-Carboxylic Acid. All ^{15}N CPMAS experiments were done on a Bruker CXP 100 pulse Fourier NMR spectrometer which was equipped with an Oxford cryomagnet with a field strength of 2.1 T and a Doty MAS probe. The resulting resonance frequencies were 90.02 MHz for ^{1}H and 9.12 MHz for ^{15}N. For the low-temperature measurements, the driving nitrogen gas was cooled with liquid nitrogen with a home-built heat-exchanger. We used a normal cross polarization sequence, which minimizes ringing artifacts,[24] with 3−8 ms cross polarization times, 6−10 μs ^{1}H-90° pulse width, 3−10 s recycle delay. The longitudinal relaxation time was measured using the pulse sequence described by Torchia,[25] without proton decoupling during relaxation period.

All spectra are referenced to external polycrystalline $^{15}NH_4Cl$. To convert these data into the nitromethane scale, we used the relation[26]

$$\delta(CH_3NO_2) = \delta(^{15}NH_4Cl_{cryst}) - 338.1 \text{ ppm} \quad (1)$$

This equation differs from the relation

$$\delta(CH_3NO_2) = \delta(^{15}NH_4Cl_{liqu}) - 352.9 \text{ ppm} \quad (2)$$

where $\delta(^{15}NH_4Cl_{liqu})$ refers to a saturated solution of $^{15}NH_4Cl$ in D_2O at 298 K.[26] The difference $\delta = (^{15}NH_4Cl_{cryst}) - \delta(^{15}NH_4Cl_{liqu}) = 17.2$ ppm arises from different intermolecular interactions.

The ^{15}N CPMAS NMR-line shape analysis of pyrazole-4-carboxylic acid was performed using procedures described previously.[27] The proton tautomerism between the two states A and B depicted in Figure 3 modulates the isotropic nitrogen chemical shifts (ν_X and ν_Y in Hz). The tautomerism is characterized by the equilibrium constant $K = k_{AB}/k_{BA} = x_B/x_A$, where k_{ij} represent the rate constants and x_i the mole fractions. Figure 3a shows the line shape contributions of the two individual nitrogen atoms X and Y as a function of an increasing rate constant k_{AB}, divided by the chemical shift difference $\Delta\nu = \nu_X - \nu_Y$. The usual features of a nondegenerate exchange process result. The sum of the two contributions gives the total line shape depicted in Figure 3b. Here, two lines are observed in the slow-exchange regime, which broaden and coalesce into two new lines exhibiting a reduced splitting $\delta\nu$ in the fast-exchange regime, given by

$$\delta\nu/\Delta\nu = (1 - K)/(1 + K) \quad (3)$$

as stated previously.[27] Figure 3c shows the well-known degenerate case with $K_{AB} = 1$, and Figure 3d shows the case of very fast exchange, where the value of the equilibrium constant K_{AB} varies from a very small value to a value of 1. Here, the two lines continually shift toward each other and can be obtained from the splitting K_{AB} according to eq 3.

Finally, Figure 3e shows the case of a superposition of different sites, all of them exhibiting a fast tautomerism, but characterized by different equilibrium constants. In this graph we assume that the site with $K_{AB} = 1$ that gives rise to the central line and the sites with $K_{AB} \approx 0$ dominate over those with intermediate values. We will show that this kind of line shape is observed for pyrazole-4-carboxylic acid at the proton disorder−order transition temperature.

Results

Crystal Structure of Pyrazole-4-carboxylic Acid (1). The compound, $C_4H_4N_2O_2$, $M_r = 112.088$, presents a tetragonal

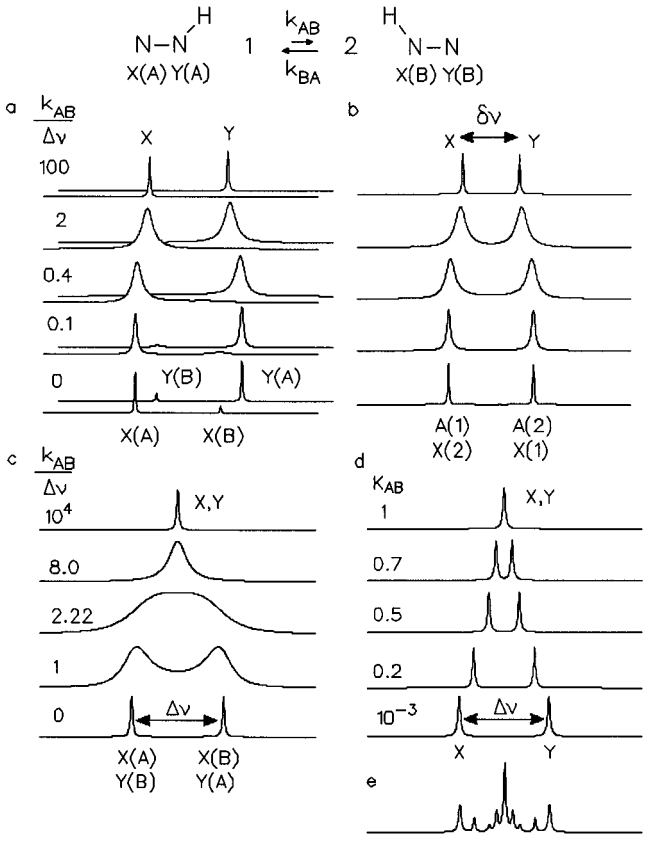

Figure 3. Simulated NMR spectra of a system of two ^{15}N spins X and Y, which exist in two states A and B. In state A a proton is bound to Y and in state B to X. The equilibrium constant is given by $K_{AB} = k_{AB}/k_{BA}$. Only the isotropic chemical shifts are taken into account, where $\Delta\nu$ corresponds to the chemical shift difference in Hz. (a) Subspectra of X and Y for the asymmetric exchange case with $K < 0$. (b) Superposed subspectra of X and Y. In the fast exchange, a splitting $\delta\nu$ is observed, given by eq 1. (c) Symmetric case with $K = 1$. (d) Asymmetric case in the fast-exchange regime with varying values of K_{AB}. (g) Arbitrary superposition of systems with different values of K_{AB}.

symmetry at both temperatures, with a space group *I*-42*d* with $Z = 8$ molecules in the unit cell, and $F(000) = 464$. At 295 K we obtained the following crystal data: $a = b = 6.8984(3)$, $c = 19.5185(24)$ Å, $D_c = 1.603$ g cm^{-3}, $\mu = 1.21$ mm^{-1}, $R(R_w) = 0.046(0.049)$ for 39 variables and 222 observed reflections [$I > 2\sigma(I)$ criterion, $\theta_{max} = 66.3°$], largest peak in the final difference synthesis of 0.57 e·Å^{-3}, goodness of fit 1.033, and maximum U33(N2) = 0.077(2) Å^2. At 150 K the following results were obtained: $a = b = 6.8872(3)$ Å, $c = 19.3571(19)$ Å, $D_c = 1.622$ gr cm^{-3}, $\mu = 1.22$ mm^{-1}, $R(R_w) = 0.053(0.066)$ for 39 variables and 241 observed reflections [$I > 2\sigma(I)$ criterion, $\theta_{max} = 65.0°$], largest peak in the final difference synthesis of 0.49 e·Å^{-3}, goodness of fit 1.014, and maximum U33(N2) = 0.068(2) Å^2. No phase transition was detected by DSC between 295 and 150 K.

The structures of **1** obtained at both temperatures are depicted in Figure 4, a and b. Although all hydrogen atoms were obtained from difference Fourier synthesis, even those of the HB (H2 and H7, with occupancy factors of 0.5) were kept fixed in the last cycles of the refinement.

The compound crystallizes in the centrosymmetric space group *I*-42*d* at both temperatures with a half-molecule in the asymmetric unit. The molecule is located on a two-fold axis; thus, only the N2, C3, C4, C6, and O7 atoms constitute the asymmetric unit. This observation implies a proton disorder of

(24) Du Bois Murphy, P. *J. Magn. Reson.* **1986**, *70*, 307.
(25) Torchia, D. A. J. *J. Magn. Reson.* **1978**, *30*, 613.
(26) (a) Witanowski, M.; Stefaniak, L.; Szymanski, S.; Januszewski, H. *J. Magn. Reson.* **1977**, *28*, 217. (b) Witanowski, M.; Stefaniak, L.; Webb, G. A. *Annual Reports on NMR Spectroscopy*, *11 B*; Academic Press: New York, 1981. (c) Martin, G.; Martin, M. L.; Gouesnard, J. P., *NMR: Basic Principles and Progress*; Springer: Heidelberg, Germany, 1989; Vol. 18, ^{15}N NMR Spectroscopy. (d) Srinivasan, P. R.; Lichter, R. L. *J. Magn. Reson.* **1977**, *28*, 227.
(27) (a) Wehrle, B.; Zimmermann, H.; Limbach, H. H. *J. Am. Chem. Soc.* **1988**, *110*, 7014. (b) Wehrle, B.; Limbach, H. H. *Chem. Phys.* **1989**, *136*, 223.

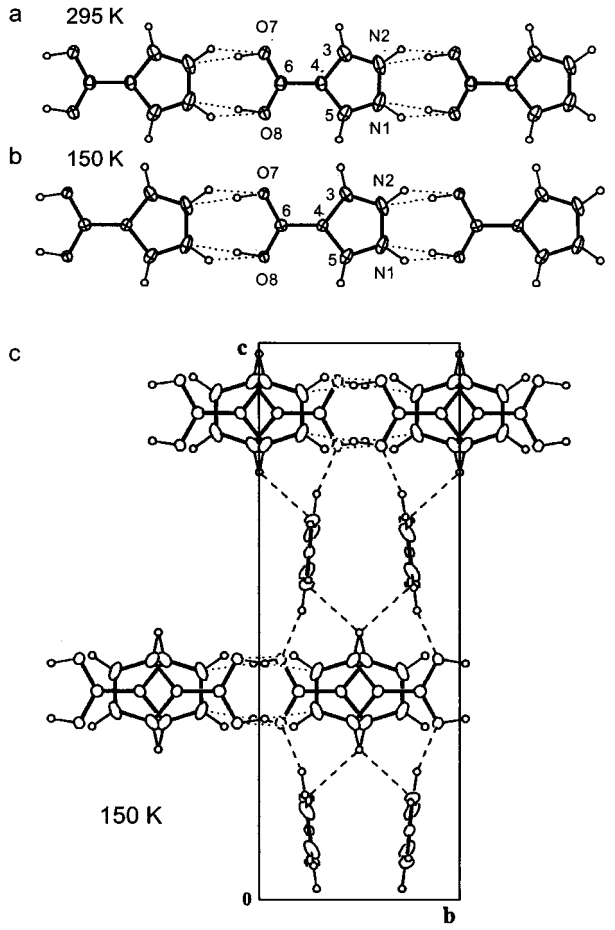

Figure 4. X-ray crystal structures of pyrazole-4-carboxylic acid chains at (a) 295 K and (b) 150 K. Thermal ellipsoids are drawn at 30% probability level. A proton disorder is observed, which implies that each bridge has a probability of 0.5 of existing either as an almost linear O−H···N or a nonlinear O···H−N hydrogen bond. The hydrogen bond parameters at 150 K are given by O7−H7···N2(−1 + *x*,*y*,*z*), *d*(O···N)= 2.746(4) Å, *d*(H···N) = 1.80 Å, and OHN angle 175°. (c) Crystal packing of the 150 K structure along **a** showing the C3−H3...O7(Y, 1 − *x*,1 − *z*) interactions between sheets. *d*(C···O) = 3.196-(4) Å, *d*(H···O) = 2.58 Å, and OHN angle 121°.

the N−H and O−H groups. The main differences between both structures, at 295 and 150 K (Figure 4, a and b), are found in the O7 (*z* coordinate and U22 and U33 displacement parameters) and N2 atoms (U22 displacement parameter), as tested by normal probability plots.[28] The displacement parameters at N2 reflect the differences between the internal angles at the nitrogen atom in the nondisordered compounds as the pyrazole itself,[1a] the C−NH−N angle being greater than the N−N═C angle [113.0(5) vs 103.7(5)° as determined at 108 K].

Hydrogen bonding involving the carboxylic acid and the nitrogen atoms of the pyrazole occurs between molecules related by translation along the **c** axis, forming O−H···N and O···H−N hydrogen-bonded chains. The chains pack to form sheets by stacking interactions along the **a** and **b** directions as indicated in Figure 4c. The angle between the chains is 14.0(2)°, and the distance from the C4 atom to the pyrazole plane is 3.418(1) Å. The perpendicular sheets are linked by weak C3−H3···O7 interactions (Figure 4c).

NMR Measurements. When we recorded the first room temperature ^{15}N CPMAS NMR spectrum of **1** (which turned out to be a metastable amorphous form), we observed a line

(28) Abrahams, S. C.; Keve, R. T. *Acta Crystallogr*. **1972**, *A28*, 215.

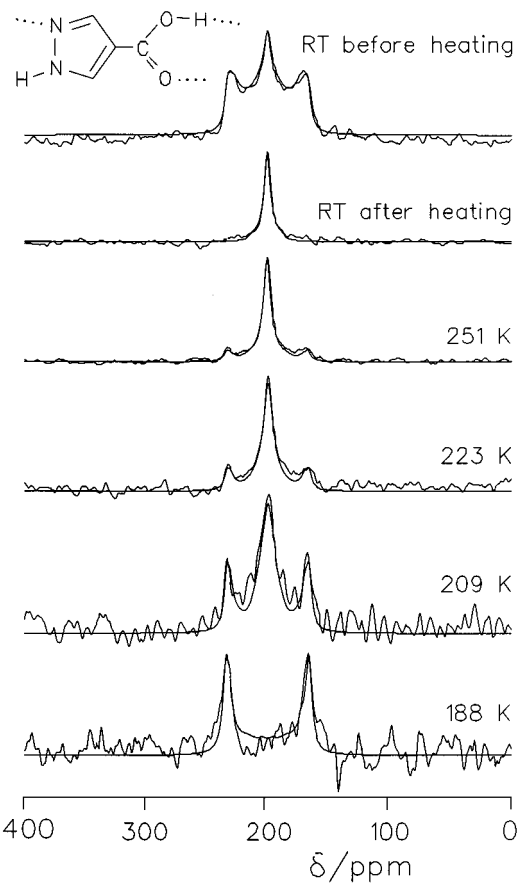

Figure 5. ^{15}N CPMAS-spectra of pyrazole-4-carboxylic acid obtained under various conditions.

trio centered at 202.7 ppm, as indicated at the top of Figure 5. The trio corresponds to a superposition of at least two nitrogen sites, one characterized by the equilibrium constant of tautomerism $K_{AB} \approx 0$ and the other by $K_{AB} \approx 1$. However, a significant line intensity between the lines of the trio indicated additional sites with $0 < K_{AB} < 1$. When we heated the sample to about 100 °C for about 1 h in the NMR spectrometer and recorded the spectrum at this temperature, a single central line was observed. However, when the sample was measured again at room temperature, the trio had disappeared (Figure 5, second spectrum from the top), and only the central line had survived. This indicated to us that the initial sample corresponded to a metastable amorphous phase. The subsequent studies were then performed on the annealed sample to which we assigned a polycrystalline structure.

When we cooled this sample to low temperatures, we again observed the appearance of outer lines corresponding to sites with $K_{AB} \approx 0$, which coexist with sites characterized by intermediate K_{AB} values, and values with $K_{AB} \approx 1$. We assign this change to a high-order phase transition of the crystal extending over a large range of temperatures. Now, we found that the temperature-induced line shape changes were reproducible.

Line shape calculations were then performed to extract the distribution of equilibrium constants K_{AB} of the tautomerism. For this purpose, we took 20 arbitrarily chosen sites into account. Each site was characterized by a given equilibrium constant between 0 and 1, where each site contributes two Lorentzian nitrogen signals. The probability $P(K_{AB})$ of finding a certain value of K_{AB} derived from the spectra of Figure 5 is plotted in Figure 6.

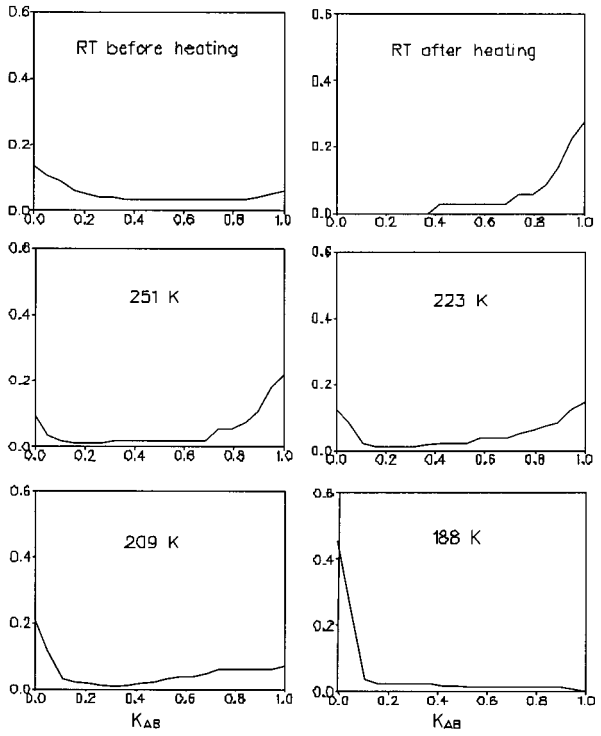

Figure 6. Distribution of K_{AB} values of proton transfer in solid pyrazole-4-carboxylic acid as a function of temperature.

Results of the ab Initio Calculations. The calculated energies of the various pyrazole-4-carboxylic acid associates are gathered in Table 1. The results indicate that the AB monomer is less stable than the AA monomer, but the energy difference is only 0.15 kcal mol^{-1}. A similar situation is observed in the case of the dimers and trimers, where all the structures are within 0.12 and 0.16 kcal mol^{-1}, respectively. The same happens in the calculated tetramers, pentamers, and heptamers, where the energy ranges are 0.13, 0.10, and 0.21 kcal mol^{-1}, respectively. These small differences indicate the quasi-degeneracy of all the possible structures. In addition, the small energetic differences observed cannot be easily rationalized on the basis of the disposition of smaller cluster or monomers.

In each cluster, a pair of coupled O···H−N and O−H···N hydrogen bonds are formed. The final geometry of each pair is a compromise to optimize the energy. Thus, while the N···H distance (1.776 ± 0.003 Å) is slightly shorter than the O···H one (1.840 ± 0.003 Å), the corresponding nitrogen−oxygen distances are almost identical, that is, 2.773 ± 0.003 Å. By contrast, the hydrogen-bond angles are very different, that is, 149.2 ± 0.2° for the O···H−N and 171.1 ± 0.0° for the O−H···N hydrogen bond. The lack of symmetry in the pyrazole molecules in the direction of the chain produces a small bend in the AAAA... disposition, while the ABAB... structures are almost linear due to a compensation effect. For the AAAA trimer, this angle is only 178.3°. In larger chains, the cumulative effect is noticeable, as illustrated for the heptamer in Figure 7a. If one composes a larger ribbon from heptamers, a circle of about 200 molecules is obtained, of which one-fourth is illustrated in Figure 7b. However, a perfectly linear ribbon results from heptamers in the ...ABABA...structure, as illustrated in Figure 7, c and d.

Discussion

The structure of pyrazole-4-carboxylic acid in the solid state is an interesting case. We studied it using X-ray crystallography, solid-state NMR and ab initio calculations. The X-ray structure of this molecule (Figure 4) showed a linear ribbon with half-proton densities on the oxygen and nitrogen atoms. Using this method, we observed almost no temperature effects on the structure. The same holds for differential scanning calorimetry. On the other hand, high-resolution ^{15}N solid-state NMR showed a dynamic disorder of the hydrogen-bonded protons at room temperature, leading to a single type of nitrogen atoms. However, by cooling to 200 K and below, a complicated disorder−order transition is observed, leading eventually to two types of nitrogen atoms, that is, hydrogen bonds, an O−H···N and an O···H−N hydrogen bond (see Figure 5). At the transition temperature of about 210 K, both the disordered hydrogen bonds and the two ordered hydrogen bonds are observed in slow exchange. A similar phase was observed when the sample was precipitated rapidly from water.

For a long time, we had great difficulty finding a scenario to accommodate these findings. It was only when we realized that an O···H−N hydrogen bond can be less linear or longer than an O−H···N hydrogen bond, as illustrated in Figure 2, that we realized that longer pyrazole-4-carboxylic acid ribbons may also exhibit nonlinear superstructures as illustrated in Figure 2. Accordingly, we applied ab initio calculations of pyrazole-4-carboxylic acid associates to verify this hypothesis. We were surprised to find that the two tautomeric states of each carboxylic acid-pyrazole link exhibit very similar energies, which are affected only slightly by the tautomeric states of the neighboring links (Table 1). On the other hand, the calculated structure of heptamers does indeed exhibit either a curved ribbon structure as in Figures 2b and 7a for the all-*anti* conformation and an undulated ribbon structure as in Figures 2c and 7c for the all-*syn* conformation. This result indicates that it is energetically more favorable to have both a quasi-linear O−H···N hydrogen bond and a somewhat longer, nonlinear O···H−N hydrogen bond with localized protons in each molecular link than two hydrogen bonds exhibiting the same geometry and a degenerate proton motion. However, the calculated energy differences are small.

Table 1. Total and Relative Calculated Energies of the Pyrazole-4-carboxylic Acid Monomers and Associates

associate	structure	total energy (hartree)	relative energy (kcal mol^{-1})
monomer	AA	−414.773899	0.00
monomer	AB	−414.773668	0.11
dimer	AAA	−829.576627	0.03
dimer	AAB	−829.576490	0.12
dimer	ABB	−829.576679	0.00
dimer	ABA	−829.576635	0.03
trimer	AAAA	−1244.379413	0.09
trimer	AAAB	−1244.379305	0.16
trimer	AABB	−1244.379468	0.06
trimer	AABA	−1244.379419	0.09
trimer	ABBB	−1244.379514	0.03
trimer	ABBA	−1244.379439	0.08
trimer	ABAA	−1244.379563	0.00
trimer	ABAB	−1244.379507	0.03
tetramer	AAAAA	−1659.182255	0.11
tetramer	AAABA	−1659.182217	0.13
tetramer	AABBA	−1659.182225	0.12
tetramer	AABAA	−1659.182345	0.05
tetramer	ABBBA	−1659.182261	0.10
tetramer	ABBAA	−1659.182385	0.02
tetramer	ABAAA	−1659.182423	0.00
tetramer	ABABA	−1659.182386	0.02
pentamer	AAAAAA	−2073.985056	0.10
pentamer	ABABAB	−2073.985217	0.00
heptamer	AAAAAAAA	−2903.590712	0.21
heptamer	ABABABAB	−2903.591052	0.00

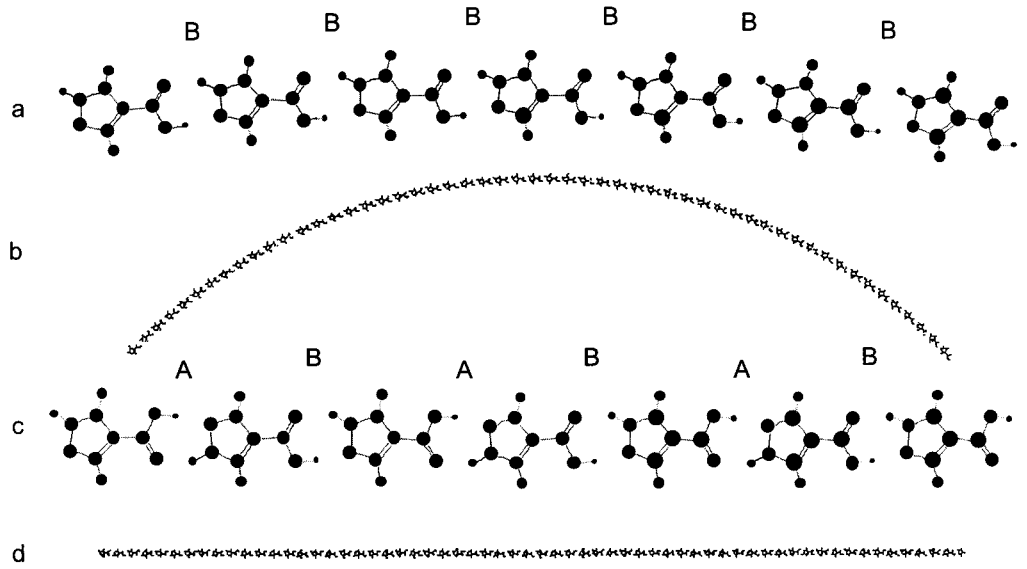

Figure 7. Optimized geometries of pyrazole-4-carboxylic acid heptamers. (a) AAAAAAA type. (b) About 216 molecules with A-links form a circle, of which one-fourth is depicted. (c) A ABABABA heptamers. (d) Undulated chain of pyrazole-4-carboxylic acid molecules consisting of alternating A and B links.

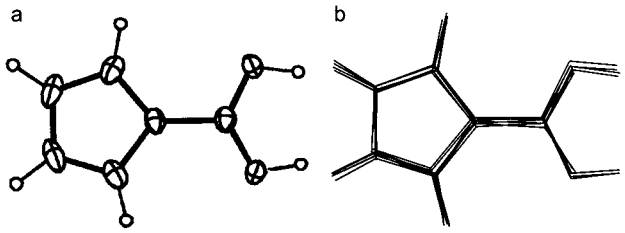

Figure 8. Comparison of the crystal structure (a) of pyrazole-4-carboxylic acid at 150 K with (b) the superposed calculated structures of the heptamer exhibiting the undulated ribbon structure shown in Figure 7d.

In Figure 8, a and b we compare the average X-ray crystal structure of pyrazole-4-carboxylic acid with the geometries of the seven superposed molecules of the heptamer of the undulated ribbon depicted in Figure 7c. It is clear that the variations of the atomic positions along the undulated ribbon are very small. Hence, the difference between the linear ribbon with a statistical sequence of tautomeric states A and B along the ribbon and the undulated linear ribbon with a strongly alternating sequence ...ABABA...could not be detected by X-ray crystallography. This explains why we did not see different molecular X-ray structures at 295 and 150 K. However, as indicated in Figure 2, a transition between the two phases is accompanied by a localization of the protons, that is the separation of the hydrogen bonds into O−H···N and O···H−N hydrogen bridges. This explains the disorder−order transition from equivalent nitrogen atoms both with a proton density of 0.5 at high temperatures to two kinds of nitrogen atoms, one protonated and the other nonprotonated, at low temperatures, as shown in Figure 5. This transition occurs only at low temperature, as the energy difference between the linear ribbon and the undulated ribbon is very small.

The transition between the two phases is complicated; it starts in a noncorrelated way in different segments of a ribbon. If two ordered segments meet, they may be matched or not-matched; for example, a defect of the type ...ABABABBA-BABA... may be created. On the other hand, if there is a distribution of ribbons of different length in the polycrystalline material, the temperature of the disorder−order transition understandably depends on the chain length, which might

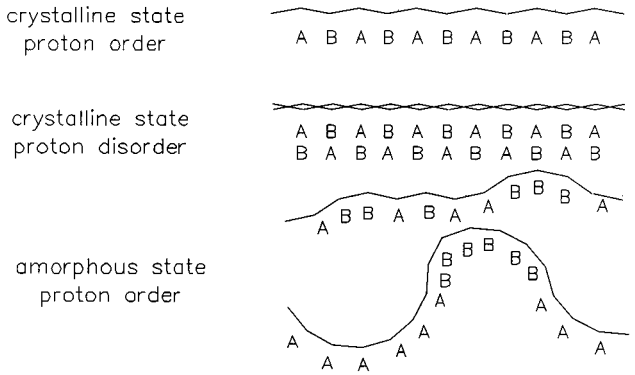

Figure 9. Schematic structure of hydrogen-bonded ribbons of pyrazole-4-carboxylic acid in the solid state. (Top) Linear undulated ribbon in the crystalline state at low temperature exhibiting an alternating sequence of nonequivalent shorter O−H···N and longer O···H−N hydrogen bond pairs (proton order). (Center) Linear ribbon in the crystalline state exhibiting equivalent fast interconverting O−H···N and O···H−N hydrogen bonds at room temperature (proton disorder). (Bottom) Curved ribbons exhibiting a nonalternating sequence of O−H···N and O···H−N hydrogen bond pairs leading to more or less curved ribbons in the amorphous state.

explain the NMR finding that both ordered and disordered segments are observed at around 200 K.

We can now also offer an explanation for the observation of a large amount of ordered pyrazole-4-carboxylic acid molecules (Figure 5, top spectrum) when the compound is precipitated rapidly from water. Within the framework of a curved or undulated structure for a ribbon with ordered protons, it is conceivable that ribbons are formed, exhibiting not strongly alternating O−H···N and O···H−N hydrogen bond pairs, as illustrated schematically at the bottom of Figure 9. When the material is annealed, the polycrystalline state exhibiting the linear ribbon structure with disordered protons is reached (center). At low temperatures the undulated ribbon structure eventually forms, again exhibiting ordered protons (top).

Conclusions

We conclude that the case of solid pyrazole-4-carboxylic acid is a very complicated, but interesting, case of a bifunctional

molecule with two proton donors and two proton acceptors which allows the formation of a molecular linear ribbon in the solid state in which each molecule is involved in four NHO-hydrogen bonds. Moreover, the protons in these hydrogen bonds are mobile and disordered at room temperature, consistent with a degenerate tautomerism and a single type of fast interconverting O−H···N and O···H−N hydrogen bonds. At low temperatures proton ordering takes place. This process seems to be driven by the tendency of O−H···N hydrogen bond to be stronger, shorter, or more linear than the corresponding O···H−N hydrogen bond. This phenomenon is associated with a curvature of hydrogen-bonded pyrazole carboxylic acid ribbons in the gas phase or with an undulated linear ribbon structure in the crystal at low temperatures. Thus, the proton-transfer equilibrium detected by ^{15}N solid-state NMR is a sensitive tool for studying molecular structure that cannot easily be detected by X-ray crystallography. The complicated experimental results were only interpreted with the help of ab initio calculations.

Currently, we are using ^{15}N- and ^{2}H relaxometry to study the dynamics of the proton and the corresponding deuteron motions, which produce interesting kinetic data, including isotope effects. These results will be reported in a future paper, which will also discuss the barrier of the double proton transfer in pyrazole-carboxylic acid links compared to carboxylic acid and pyrazole dimers.

Acknowledgment. We thank the European Community, Brussels (Project no. CHRX-CT940582), the Deutsche Forschungsgemeinschaft, Bonn-Bad Godesberg, the Fonds der Chemischen Industrie, Frankfurt, and the Spanish DGICYT (PB96-0001-C03) for financial support. Computational resources of the Computing Center of the Freie Universität Berlin are acknowledged.

JA002688L